SHAPE OPTIMIZATION

OF

ELASTIC BARS IN TORSION

Jean W. Hou, Edward J. Haug, and Robert L. Benedict

Center for Computer Aided Design
College of Engineering
The University of Iowa
Iowa City, Iowa 52243

ABSTRACT

The problem of shape optimal design for multiply-connected elastic bars in torsion is formulated and solved numerically. A variational formulation for the equation is presented in a Sobolëv space setting and the material derivative idea of Continuum Mechanics is used for the shape design sensitivity analysis. The finite element method is used for a numerical solution of the variational state equation and is integrated into an iterative optimization algorithm. Numerical results are presented for both simply- and doubly-connected bars, with prescribed bounds on admissible location of both inner and outer boundaries.

ACKNOWLEDGEMENT

This research was supported by NSF Grant No. CEE 80-05677.

INTRODUCTION

The use of material derivative in the so called "speed method" was introduced by J. Cea, J.P. Zolesio, and B. Rousselet in a series of papers. For the details see [9], [7] and [8]. Here we apply it directly to the optimization of bars in torsion, and use the finite element technique to obtain specific numerical results for multiply-connected cross sections.

Consider the torsion problem for an elastic bar shown in Figure 1. The material of the bar is homogenous and isotropic and the cross section may have a void, thus resulting in a multiply-connected domain Ω. Torsional stiffness of the bar is defined by the following boundary-value problem for the stress function z (See reference [1]):

$$\left.\begin{aligned} \Delta z &= -2, \quad \text{in } \Omega \\ z &= 0, \quad \text{on } \Gamma_o \\ z &= q, \quad \text{on } \Gamma_i \end{aligned}\right\} \qquad \begin{matrix} (1) \\ (2) \\ (3) \end{matrix}$$

$$\int_{\Gamma_i} \frac{\partial z}{\partial n}\, dS = -2A_i \,, \qquad (4)$$

where Γ_o is the outer boundary of Ω and Γ_i is the inner boundary, enclosing the domain Ω_i. Here, the constant q is to be determined as part of the solution to the problem and A_i is the area of Ω_i. As shown in [1] the torsional rigidity is then given by

$$K = 2\iint_{\Omega} z \, d\Omega + 2qA_i = - \iint_{\Omega} x \cdot \nabla z \, d\Omega \quad , \tag{5}$$

where x is a position vector in Ω.

Polya and Weinstein [2], have proved the following assertion: "Of all doubly-connected cross sections with given areas of Ω and Ω_i, the ring bounded by two concentric circles has the maximum torsional rigidity."

Banichuk [3] and Kurshin and Onoprienko [4] have also investigated optimal shape of a bar with doubly-connected cross section. They hold the inner boundary Γ_i fixed and seek a shape for the outer boundary that maximizes torsional rigidity. The area of Ω is given. In addition to Equations 1-4, they obtain the following optimality condition for Γ_o:

$$\frac{\partial z}{\partial n} = C, \quad \text{on } \Gamma_o \quad . \tag{6}$$

Taking account of this excess condition, the boundary Γ_o is then determined so that the constant C matches the isoparametric constraint on area of Ω; i.e., the problem is treated as an inverse boundary-value problem. Banichuk uses a perturbation technique to obtain approximate solutions of this problem. He is able also to deduce some properties of an optimum contour. For example, wall thickness of the bar of optimum shape decreases as one moves along the inner boundary Γ_i in a direction of increasing curvature.

By restricting the cross section to be symmetric with respect to the coordinate axes, Kurshin and Onoprienko apply complex variable theory and solve Equations 1-6, with an isoparametric condition on the area of Ω. A system of nonlinear equations is obtained to determine the unknown coefficients of a complex function that describes the unknown boundary Γ_o. This system is solved by the Newton-Raphson method. Some numerical results are presented.

Quite recently, Dems [5] used a boundary perturbation analysis for a bar with doubly-connected cross section to maximize torsional rigidity, with the inner boundary held fixed. The optimality criteria obtained is the same as Equation 6. The shape optimization problem is formulated by defining shape of the boundary with a set of parameter-dependent, piecewise linear functions. The reduced problem is solved by means of the finite element method and an iterative algorithm based on the optimality condition. Several numerical examples are included.

The discussion thus far has focused on doubly-connected bars. If the cross section of the bar is simply-connected, Γ_i is a point ($A_i = 0$), and the value of q

is immaterial. Thus, the boundary-value problem for the stress function z reduces to Equations 1 and 2 on the simply-connected domain Ω and the torsional rigidity is given by Equation 5. It is interesting that Equation 6 remains valid as an optimality criterion for the shape of Ω to maximize K with a given area of Ω [3].

Difficulties in solving the torsion problem for a bar with a doubly-connected cross section are associated with the boundary conditions of Equations 3 and 4. Usually, q in Equation 3 is determined from Equation 4. However, once an admissible function space and variational formulation can be defined, it is seen that Equation 4 becomes a defining equation for a natural boundary condition. Therefore, the Finite Element technique can be employed to solve the problem numerically. In section 2, such a variational formulation and admissible function space are defined and the equivalence between the variational formulation and the Equations 1-4. We also prove the existence and uniqueness of the solution.

In section 3, the material derivative concept is employed to obtain the directional derivative of torsional rigidity with respect to the shape of the domain by allowing both Γ_i and Γ_o to vary. Optimality criteria for the simply- and doubly- connected domains are obtained.

An iterative numerical method for optimizing shape of simply- and doubly-connected shaft cross sections is outlined in Section 4. Numerical calculations are carried out using the finite element method for analysis of the designs and a nonlinear programming method for optimization. Examples of both simply- and multiply-connected bars, with constraints on admissible location of the boundaries Γ_i and Γ_o, are presented in Section 5.

2. VARIATIONAL FORMULATION OF BOUNDARY-VALUE PROBLEMS

Suppose Ω is a doubly-connected open set in R^2, bounded by regular boundaries Γ_i and Γ_o. The outer normals of the boundary curves are represented by n. The following bilinear and linear forms play a key role in the variational formulation of the problem:

$$a(z, v) = \int_{\Omega} \nabla z \cdot \nabla v \, d\Omega \tag{7}$$

$$(x, \nabla v) = \int_{\Omega} x \cdot \nabla v \, d\Omega \tag{8}$$

where $x \in \Omega \subset R^2$ is a position vector, ∇ denotes the gradient operator, and $x \cdot u = x_1 u_1 + x_2 u_2$. The variational equation for the torsion problem is given by:

$$a(z, v) + (x, \nabla v) = 0, \quad \text{for all } v \in V, \tag{9}$$

where

$$V = \{v \in H^1(\Omega) \mid v = 0 \text{ on } \Gamma_o \text{ and } v = \beta \text{ on } \Gamma_i, \text{ for some } \beta \in R^1\} ,$$

and where $H^1(\Omega)$ is the Sobolev space of order one [6].

One may define a formal operator Λ as, $\Lambda w(x) = -\Delta w(x)$, where $x \in \Omega$ and Δ is the Laplace operator. The domain of this formal operator is defined as

$$H^1(\Omega, \Lambda) = \{w \in H^1(\Omega) \mid \Lambda w \in L^2(\Omega)\} \tag{11}$$

Moreover, one may define the function space

$$V(\Lambda) = \{w \in H^1(\Omega, \Lambda) \mid w = 0 \text{ on } \Gamma_o \text{ and } w = \beta \text{ on } \Gamma_i \text{ , for some } \beta \in R^1\} \tag{12}$$

In the definitions of spaces in Equations 10-12, a function w evaluated on a boundary Γ is interpreted as a trace γw defined in $H^{\frac{1}{2}}(\Gamma)$ (See [6]). One may proceed to prove the following proposition:

Proposition. The following problems are equivalent:
Problem (a); Find $z \in H^1(\Omega, \Lambda)$ and $q \in R^1$ to satisfy

$$\Lambda z = 2, \quad \text{in } \Omega \tag{13}$$

$$z = 0, \quad \text{on } \Gamma_o \tag{14}$$

$$z = q, \quad \text{on } \Gamma_i \tag{15}$$

$$\int_{\Gamma_i} \frac{\partial z}{\partial n}\, dS + \int_{\Gamma_i} x \cdot \mathbf{n}\, dS = 0 \quad , \tag{16}$$

where $\int_{\Gamma_i} x \cdot \mathbf{n}\, dS$ is equal to twice of area enclosed in Γ_i.

Problem (b); Find $z \in V$ such that

$$a(z, v) + (x, \nabla v) = 0, \text{ for all } v \in V \ . \tag{17}$$

Proof:

(a → b). Suppose $z \in H^1(\Omega, \Lambda)$ is a solution of problem (a). Then, $z \in V(\Lambda)$. Since $z \in V(\Lambda) \subset H^1(\Omega, \Lambda)$ and $v \in V \subset H^1(\Omega)$, Green's formula for $z \in V(\Lambda)$ and any $v \in V$, is (as given in [6])

$$\begin{aligned} a(z, v) &= (\Lambda z, v) + \langle \delta z, \gamma v \rangle \\ &= (2, v) + \int_{\Gamma_i \ \Gamma_o} \frac{\partial z}{\partial n}\, v\, dS \\ &= (2, v) + \beta \int_{\Gamma_i} \frac{\partial z}{\partial n}\, dS \end{aligned} \tag{18}$$

where $\delta z \in H^{-1/2}(\Gamma)$ is an extension of $\frac{\partial z}{\partial n}$. The second and third equalities in Equation 18 are deduced from the facts that $\Lambda z = 2$ in Ω, $v = 0$ on Γ_0, and $v = \beta$ on Γ_i, for some constant β. Further, div $x = \nabla \cdot x \equiv 2 \in L^2(\Omega)$. Hence, $x \in H^1(\Omega, \text{div}) = \{u \in L^{2,2}(\Omega) \mid \text{div } u \in L^2(\Omega)\}$ and

$$(x, \nabla v) = -(2, v) + \int_{\Gamma_i \cup \Gamma_0} x \cdot n \, v \, dS$$

$$= -(2, v) + \beta \int_{\Gamma_i} x \cdot n \, dS \tag{19}$$

Adding Equations 18 and 19 and using Equation 16, it follows that

$$a(z, v) + (x, \nabla v) = \beta\left(\int_{\Gamma_i} x \cdot n \, dS + \int_{\Gamma_i} \frac{\partial z}{\partial n} \, dS\right) = 0 \tag{20}$$

for all $v \in V$. Thus, z is a solution of Problem (b).

(b $\rightarrow$ a). Suppose $z \in V$ is a solution of Problem (b). Since $z \in V$, the boundary conditions in Equations 14 and 15 of Problem (a) are satisfied. One may first consider only those $v \in V$ such that $v = 0$ on Γ_i; i.e., $v \in H_0^1(\Omega) \subset V \subset H^1(\Omega)$. Recall that $z \in V \subset H^1(\Omega)$ and $x \in H^1(\Omega, \text{div})$. For this class of v, Green's formula (see [6]) is

$$a(z, v) = (\Lambda z, v) \quad , \tag{21}$$

where $\Lambda z \in H^{-1}(\Omega)$ and

$$(x, \nabla v) = (-2, v) \quad . \tag{22}$$

Adding Equations 21 and 22, it follows that

$$a(z, v) + (x, \nabla v) = (\Lambda z - 2, v)$$

for all $v \in H_0^1(\Omega)$. It is given that the left side of this equality vanishes, so $(\Lambda z - 2, v) = 0$ for all $v \in H_0^1(\Omega)$. This implies that $\Lambda z - 2 = 0$ in $H^{-1}(\Omega)$. But $\Lambda z = 2 \in L^2$, so it follows that $z \in H^1(\Omega, \Lambda)$. Since $z \in H^1(\Omega, \Lambda)$, Green's formula is valid for all $v \in V \subset H^1(\Omega)$, giving

$$a(z, v) = (\Lambda z, v) + \int_{\Gamma_i \cup \Gamma_0} \frac{\partial z}{\partial n} \, v \, dS$$

$$= (\Lambda z, v) + \beta \int_{\Gamma_i} \frac{\partial z}{\partial n} \, dS \quad .$$

and

$$(x, \nabla v) = (-2, v) + \int_{\Gamma_i \cup \Gamma_o} x \cdot \mathbf{n}\, dS$$

$$= (-2, v) + \beta \int_{\Gamma_i} x \cdot \mathbf{n}\, dS$$

Adding, it follows that

$$a(z, v) + (x, \nabla v) = (\Lambda z - 2, v) + \beta \left[\int_{\Gamma_i} \left(\frac{\partial z}{\partial n} + x \cdot \mathbf{n}\right) dS\right], \text{ for all } v \in V .$$

The left side of this equation vanishes and it was shown that $\Lambda z = 2$, so

$$\beta \int_{\Gamma_i} \left(\frac{\partial z}{\partial n} + x \cdot \mathbf{n}\right) dS = 0$$

for all $v \in V$, equivalently for any $\beta \in R^1$. Thus,

$$\int_{\Gamma_i} \left(\frac{\partial z}{\partial n} + x \cdot \mathbf{n}\right) dS = 0$$

and the last condition (Equation 16) of Problem (a) is satisfied. Q.E.D.

One may define $\hat{\Omega} = \Omega \cup \Omega_i \cup \Gamma_i$ and extend the function $z \in V(\Omega)$ to z in $\hat{\Omega}$, with the definition

$$z = \begin{cases} z, & \text{in } \Omega \\ q \in R^1, & \text{in } \Omega_i \cup \Gamma_i \end{cases} .$$

An example of such a function is shown in Figure 2. This extended function belongs to $H_0^1(\hat{\Omega})$. For all $v \in H_0^1(\hat{\Omega})$, Poincare's inequality implies that

$$\int_{\hat{\Omega}} (\nabla v \cdot \nabla v) d\Omega > \alpha \int_{\hat{\Omega}} v^2\, d\Omega ,$$

where $\alpha > 0$. Adding $\hat{a}(v, v) \equiv \int_{\hat{\Omega}} \nabla v \cdot \nabla v\, d\Omega$ to both sides of the above inequality

and dividing by two, one has

$$\hat{a}(v, v) > \frac{\alpha}{2} \int_{\hat{\Omega}} v^2 \, d\Omega + \frac{1}{2} \int_{\hat{\Omega}} (\nabla v \cdot \nabla v) d\Omega$$

$$> \min \left(\frac{\alpha}{2}, \frac{1}{2}\right) ||v||^2_{H_0^1(\hat{\Omega})} \quad . \tag{23}$$

It is evident that $c = \min(\alpha/2, 1/2)$ is greater than zero for $\alpha > 0$. Because z is constant in Ω_i, $\nabla z = 0$ in Ω_i. Therefore,

$$\hat{a}(z, z) = \int_{\hat{\Omega}} \nabla z \cdot \nabla z \, d\Omega$$

$$= \int_{\Omega} \nabla z \cdot \nabla z \, d\Omega = a(z, z) \quad .$$

Furthermore,

$$||z||^2_{H_0^1(\hat{\Omega})} = ||z||^2_{V(\Omega)} + q^2(\text{mes } \Omega_i)$$

$$> ||z||^2_{V(\Omega)} \quad .$$

Substituting these results into Equation 23, one finally has $c > 0$ and

$$a(z, z) > c \, ||z||^2_V, \quad \text{for all } z \in V \quad . \tag{24}$$

Having proved V-ellipticity of a(z, z) (Equation 24), the Lax-Milgram Theorem (as used in [6]) ensures existence and uniqueness of a solution of the Problem (b). The proposition proved above implies that this solution is the unique solution of Problem (a).

3. SHAPE DESIGN SENSITIVITY ANALYSIS

Since the domain Ω is to be varied, it is convenient to treat it as a continuum and utilize the idea of material derivative, as introduced in continuum mechanics, to find the domain variation of the functionals concerned. One method of defining a variation in the domain Ω is to let $V(X)$, $X \in \Omega$, be a vector field that may be thought of as a "design velocity". A one parameter family perturbed domain may then be defined by the mapping

$$x = X + tV(X), \quad X \in \Omega, \; t \in R^1 \tag{25}$$

One may denote the deformed domain as $\Omega(t)$, with $x \in \Omega(t)$.

If z is the solution of Equation 17, which depends on the shape of $\Omega(t)$, then z depends on t both through the position $x = X + tV(X)$ and explicitly; i.e., $z = z(x, t)$. Under certain regularity hypothesis on Ω and the vector field V(X) [7,8], one can define

$$\dot{z}(X) \equiv \lim_{t \to 0} \left[\frac{z(X+tV) - z(X)}{t}\right]$$

$$= z'(X) + \nabla z(X) \cdot \Lambda(X) \tag{26}$$

where $\dot{z}$ is the material derivative and z' is the partial derivative, defined as

$$z'(X) \equiv \lim_{t \to 0} \left[\frac{z(X, t) - z(X, 0)}{t}\right] \tag{27}$$

If $z \in H^1(\Omega)$, with smoothness assumptions on the domain and velocity field V(X) [7], then $z' \in H^1(\Omega)$ [9], and $\dot{z} \in H^1(\Omega)$ [7, 8]. Thus, $(\nabla z \cdot V) \in H^1(\Omega)$. It is shown in References 7-9 that the following properties of the material derivative, which are well known in continuum mechanics, are valid in the Sobolev space setting:

$$(\nabla z)' = \nabla(z') \tag{28}$$

and for an integral functional

$$\dot{\Phi} = \iint_{\Omega} F(z, x) \, d\Omega \tag{29}$$

the material derivative is

$$\dot{\Phi} = \iint_{\Omega} \frac{\partial F}{\partial z} z' \, d\Omega + \int_{\Gamma_i \cup \Gamma_o} F \, V_n \, dS \tag{30}$$

where $V_n = V \cdot n$ is the normal component of V on the boundary of Ω.

More fundamental is the question of existence of the material and partial derivatives $\dot{z}$ and z' of the solution z of the variational equation of Equation 17. Under hypotheses of strong ellipticity of the energy bilinear form $a(\cdot, \cdot)$, proved in Equation 24, it is shown in References 8-10, that z is differentiable with respect to shape. With this knowledge and the material derivative formulas of Equations 26, 28, and 30, one can now study the torsional shape optimal design problem.

The first order domain variation of torsional rigidity is, from Equation 5 and 30,

$$\dot{K} = -(x, \nabla z') - \int_{\Gamma_i \cup \Gamma_o} x \cdot \nabla z \, V_n \, dS \tag{31}$$

Selecting v = z in Equation 17, one has,

$$a(z, z) + (x, \nabla z) = 0 \ . \tag{32}$$

Taking the material derivative of both sides of this equation gives

$$2a(z, z') + (x, \nabla z')$$

$$= - \int_{\Gamma_i \cup \Gamma_o} \nabla z \cdot \nabla z \, V_n \, dS - \int_{\Gamma_i \cup \Gamma_o} x \cdot \nabla z \, V_n \, dS \ . \tag{33}$$

Since $z' \in H^1(\Omega)$ and $\nabla z = -2$ in Ω, Green's formula yields

$$a(z, z') + (x, \nabla z') = (2, x') + \int_{\Gamma_i \cup \Gamma_o} \frac{\partial z}{\partial n} \, z' \, dS$$

$$+ (-2, z') + \int_{\Gamma_i \cup \Gamma_o} (x \cdot n \, z') dS$$

$$= \int_{\Gamma_i \cup \Gamma_o} \frac{\partial z}{\partial n} z' \, dS + \int_{\Gamma_i \cup \Gamma_o} (x \cdot n \, z') dS \ .$$

Substituting this result into Equation 33, it follows that

$$2 \int_{\Gamma_i \cup \Gamma_o} \frac{\partial z}{\partial n} z' \, dS + 2 \int_{\Gamma_i \cup \Gamma_o} x \cdot z' \, dS - (z, \nabla z')$$

$$+ \int_{\Gamma_i \cup \Gamma_o} \nabla z \cdot \nabla z \, V_n \, dS + \int_{\Gamma_i \cup \Gamma_o} x \cdot \nabla z \, V_n \, dS = 0 \ . \tag{34}$$

On boundaries Γ_i and Γ_o, z is a constant, so $\frac{\partial z}{\partial s} = 0$. Furthermore, on Γ_o $\dot{z} = z' + \nabla z \cdot V = 0$, because $z = 0$ on Γ_o. However, on Γ_i $z = q$, $\dot{z} = z' + \nabla z \cdot V = \dot{q}$. It thus follows that

$$z' = \begin{cases} -\frac{\partial z}{\partial n} V_n, & \text{on } \Gamma_o \\ q - \frac{\partial z}{\partial n} V_n, & \text{on } \Gamma_i \end{cases}$$

and

$$x = \nabla z = x \cdot n \frac{\partial z}{\partial n}, \text{ on } \Gamma_i \cup \Gamma_o \quad .$$

Therefore, Equation 31 becomes

$$\dot{K} = -(x, \nabla z') - \int_{\Gamma_i \cup \Gamma_o} x \cdot n \frac{\partial z}{\partial n} V_n \, dS \, , \tag{35}$$

and Equation 34 may be written as

$$-(x, \nabla z') - \int_{\Gamma_i \cup \Gamma_o} (\frac{\partial z}{\partial n})^2 V_n \, dS - \int_{\Gamma_i \cup \Gamma_o} x \cdot n \frac{\partial z}{\partial n} V_n \, dS$$

$$+ 2\dot{q} \{\int_{\Gamma_i} \frac{\partial z}{\partial n} dS + \int_{\Gamma_i} x \cdot n \, dS\} = 0 \quad . \tag{36}$$

Substituting from Equation 36 into Equation 35 and considering Equation 16, one has the desired result

$$\dot{K} = \int_{\Gamma_i \cup \Gamma_o} (\frac{\partial z}{\partial n}) V_n \, dS \quad . \tag{37}$$

Note that any monotone outward movement of the boundary; i.e., $V_n > 0$, yields an increase in K, which is to be expected. It is easy to repeat the arguments for a simply-connected domain Ω to see that Equation 37 is valid with Γ_i suppressed.

If the cross-sectional area A of the bar and the area A_i of the hole are given, isoparametric constraints on the shape of Ω are

$$\Phi = \int_{\Omega} d\Omega - A = 0 \tag{38}$$

$$\Phi_i = \int_{\Omega_i} d\Omega - A = 0 \tag{39}$$

Taking the derivative of both sides of these equations gives

$$\dot{\Phi} = \int_{\Gamma_i \cup \Gamma_o} V_n \, dS = 0 \tag{40}$$

$$\dot{\Phi}_i = \int_{\Gamma_i} V_n \, dS = 0 \tag{41}$$

The necessary condition for maximal torsional rigidity (equivalently the minimum of negative torsional rigidity), with shape variations consistent with Equations 38 and 39, is thus

$$-\int_{\Gamma_i \cup \Gamma_o} (\frac{\partial z}{\partial n})^2 V_n \, dS + \lambda \int_{\Gamma_i \cup \Gamma_o} V_n \, dS + \lambda_i \int_{\Gamma_i} V_n \, dS = 0 \tag{42}$$

for arbitrary V_n, where λ and λ_i are Lagrange multipliers corresponding to constraints of Equations 38 and 39. Under the assumption that V_n is smooth and arbitrary, provided no intersection of Γ_i and Γ_o occurs, one has the following necessary conditions of optimality:

$$-(\frac{\partial z}{\partial n})^2 + \lambda + \lambda_i = 0, \quad \text{on } \Gamma_i \tag{43}$$

$$(\frac{\partial z}{\partial n})^2 + \lambda = 0, \quad \text{on } \Gamma_o \tag{44}$$

It is clear that concentric circles for Γ_i and Γ_o satisfy these necessary conditions. This special case is proved in Reference 2.

If Γ_i is fixed, the necessary condition is only

$$-(\frac{\partial z}{\partial n})^2 + \lambda = 0, \quad \text{on } \Gamma_o \, , \tag{45}$$

which agrees with the results of Banichuk [3] and Dems [5].

Extensions of the preceding optimality conditions can be easily obtained using abstract optimization theory, in conjunction with the design sensitivity analysis results of this section. For example, if the inner boundary Γ_i is fixed and the outer boundary Γ_o is constrained to lie within some specified curve $\tilde{\Gamma}$, then at points on $\Gamma_o \cap \tilde{\Gamma}$ the only feasible variation of the domain is $V_n \leq 0$. Thus, one can prove existence of a multiplier function $\mu(X) > 0$, $X \in \Gamma_o \cap \tilde{\Gamma}$, such that Equation 42 on Γ_o becomes identified with the vanishing of the following boundary integral

$$\int_{\Gamma_o} [-(\frac{\partial z}{\partial n})^2 + \lambda + \mu(X)] V_n \, dS = 0$$

for arbitrary V_n on Γ_n. Thus, it is necessary that

$$\begin{aligned} &-(\frac{\partial z}{\partial n})^2 + \lambda + \mu(X) = 0, && \text{on } \Gamma_o \\ &\mu(X) > 0, && \text{on } \Gamma_o \cap \tilde{\Gamma} \\ &\mu(X) = 0, && \text{on } \Gamma_o/(\Gamma_o \cap \tilde{\Gamma}) \end{aligned} \qquad (46)$$

While it is interesting to derive optimality conditions that must hold on the optimum boundary, such as Equations 43-46, it is difficlut to use these conditions to construct optimum shapes. One may view the necessary conditions as part of an inverse boundary-value problem; i.e., find the boundary of Ω so that the solution of a differential equation on Ω satisfies given boundary conditions and optimality criteria, such as Equations 43-46, on the boundary Γ. The latter, excess boundary conditions may be interpreted as determining the optimum location of the boundary. Banichuk approached a special case of the problem in this fashion in Reference 3, using a perturbation technique. Such methods are, however, very complicated and require a great deal of ad-hoc work for each problem treated.

A direct iterative optimization method is presented in the next section, based on the design sensitivity results obtained in this section, parameterization of the unknown boundary, and nonlinear programming methods.

4. ITERATIVE NUMERICAL SHAPE OPTIMAL DESIGN

A typical shape optimal design problem is to choose a domain Ω to minimize a cost functional of the form

$$\Phi_0 = \iint_{\Omega} G^0(z) \, d\Omega \quad , \qquad (47)$$

subject to functional constraints

$$\Phi_i = \iint_{\Omega} G^i(z) \, d\Omega \begin{cases} = 0, \; i = 1, \ldots, k' \\ < 0, \; i = k'+1, \ldots, k \end{cases} , \qquad (48)$$

where the state z is the solution of a variational equation of the form of Equation 17. It is further required that the boundary Γ lie between Γ^+ and Γ^-, as shown in Figure 3. The latter pointwise constraints are written in the form

$$\left.\begin{aligned} d^n(\Gamma, \Gamma^+) &> 0 \\ d^n(\Gamma^-, \Gamma) &> 0 \end{aligned}\right\} \tag{49}$$

where $d^n(.,.)$ is the distance measured along the normal n to Γ, from the first to the second curve.

Using results of Equations 37, 40, and 41, each of the functionals of Equations 47 and 48 can be differentiated (linearized) to obtain

$$\delta\Phi = \int_\Gamma \Lambda^i V_n \, d\Gamma, \qquad i = 0, 1, \ldots, k \tag{50}$$

where the sensitivity coefficients Λ^i of V_n in Equations 37, 40, and 41 define variations in the cost functional and each active functional constraint.

Even though the linearized functional appearing in Equation 50 has been obtained using a variational formulation, a finite dimensional parameterization of the boundary can be introduced to reduce this linearized functional to parametric form. Presume that points on the boundary Γ are specified by a vector $r(\alpha;b)$ from the origin of the coordinate system to the boundary, as shown in Figure 4, where α is a parameter vector and b is a vector of design parameters $b = [b_1, \ldots, b_m]^T$. When the parameterization of Γ has been defined, the domain optimization problem reduces to selection of the finite dimensional vector b to minimize the cost function of Equation 47, subject to the constraints of Equations 48 and 49. The linearized form of this problem may be written in terms of variation δb by denoting

$$b = b^0 + t\delta b \ , \tag{51}$$

where b^0 is the design at a given iteration. The velocity field at the boundary is

$$V = \frac{d}{dt}\,(r(\alpha;b)) = \frac{\partial r}{\partial b}\,\delta b \ . \tag{52}$$

Taking the dot product of V with the unit outward normal to the curve Γ yields

$$V_n = n \cdot V = [n \cdot \frac{\partial r(\alpha;b)}{\partial b}]\,\delta b \ . \tag{53}$$

Here, the coefficient of δb can be calculated at each point on Γ and the result substituted into Equation 50 to obtain

$$\delta\Phi_i = [\int_\Gamma \Lambda^i \,(n \cdot \frac{\partial r}{\partial b}\,)\, dS]\delta b \equiv \ell^{i^T} \delta b \ . \tag{54}$$

More directly, the pointwise constraints on location of Γ in Equation 49 can be linearized as

$$-d^n(\Gamma(\alpha), \Gamma^+) < n(\alpha) \cdot \frac{\partial r}{\partial b}(\alpha)\, \delta b < d^n(\Gamma^-, \Gamma(\alpha)), \text{ on } \Gamma \ . \qquad (55)$$

This constraint may be implemented over Γ in several ways, the simplest being to enforce it at a grid α_j of points.

Having defined a finite dimensional parameterization of the shape optimal design problem and obtained derivatives of the cost and constraint functions with respect to design parameters, one can now apply any well known nonlinear programming algorithm to iteratively optimize the shape. In each iteration, a finite element approximate solution of the boundary-value problem is constructed and used to evaluate design derivatives of torsional stiffness, using Equations 37 and 54. More directly, Equations 40, 41, and 54 are used to calculate derivatives of Φ and Φ_i in Equations 38 and 39. Finally, the derivatives appearing in Equation 55 are calculated directly.

Numerical results presented in the following section have been obtained by a recursive quadratic programming algorithm [11] that has been proved to be globally convergent [12]. With the design derivatives calculated, however, any gradient based, nonlinear programming algorithm can be used.

5. NUMERICAL EXAMPLES

Example 1

The first example presented deals with Polya and Weinstein's proof that concentric circles define the optimum shape, if no constraints are placed on boundary location. The amount of material is given as 65 units and the area of the hole is 20 units. Both conditions are treated as isoparametric constraints. As an initial design, two concentric circles are selected with radii 4.5 and 2.0 units, respectively. A regular polygon is used to approximate the boundary, as shown in Figure 5. The radial distances b_i between the i-th vertex and the origin are chosen as design variables.

For the coarse grid model (96 elements, 64 nodes, and 16 design variables in Figure 5(a)), six iterations, requiring 7.93 CPU seconds on a PRIME 750 minicomputer, were required for convergence to the optimum shape. It took 7 iterations and 51.57 CPU seconds for the finer grid model (384 elements, 224 nodes, and 64 design variables in Figure 5(b)) to achieve convergence. A comparison between the theoretical values and the final optimum results is given in Table 1.

Example 2

As a second example, the inner boundary is fixed as an ellipse with semi-radii a = 2.5 and b = 1.0 units. The amount of material is given as 45 units. The initial estimate for the outer boundary was taken as a circle with radius 4.5 units. Thirty-five iterations and 270.1 CPU seconds on a PRIME 750 minicomputer were

equired to achieve convergence to the design shown in Figure 6. The torsional rigidity is 415.83 at the final solution, while the initial value is 604.74. These results support Banichuk's claim that wall thickness of the bar at the optimum shape decreases as one moves along the inner boundary in a direction of increasing curvature.

Example 3

As a final example, both the outer and inner boundaries are treated as design variables. In addition to the constraint on the amount of material available, the cross section of the bar is required to be in a 10 x 16 unit rectangular housing. Two finite element meshes are used for analysis. One has 384 elements, 224 nodes, and 64 design variables as in the preceding example. The second mesh has 960 elements, 528 nodes, and 96 design variables. The initial design is taken as two concentric circles of radii 5, and 2.5 units.

With given amounts of material of 85 and 110 units, numerical results are listed in Table 2. Optimum shapes, for different finite element meshes, are shown in Figures 7 and 8. Note that the corners of the housing are not filled for all examples, as one might expect. Although the values of optimum torsional rigidities are very close for the two finite element meshes, optimum shapes of the inner boundaries show significant differences. It is apparent that improved stress evaluation, which gives a better approximation of design sensitivity coefficients, has caused this deviation. It is also interesting to see that the bar with a hole has distributed the material more efficiently (has higher torsional rigidity) than the bar with a solid cross section. Calculated with a finite element model of 384 elements, 209 nodes, and 32 design variables, numerical results for the optimum design of a solid bar are listed in Table 3. The optimum shapes are shown in Figure 9.

6. CONCLUSIONS AND REMARKS

The numerical examples offered here illustrate the wide applicability of the iterative numerical schemes for shape optimal design. Note that the pattern of finite element mesh does not change during an iteration. In each iteration, new positions of boundary nodes are determined by the algorithm and the positions of interior nodes change accordingly.

The sensitivity functional, derived using the variational formulation of the state equation and material derivative, is a boundary integral that contains only the normal boundary movement (that is V_n) and the stress terms $(\frac{\partial z}{\partial n})$. Success in a numerical technique for shape optimal design depends on an accurate evaluation of these stress terms and on the representation of the boundary and its normal movement.

A more sophisticated choice of elements or of a finer mesh can be introduced in the finite element method to improve the numerical approximation of stress

values. Instead of linear piecewise functions, some smoother or more restricted classes of functions may be used to describe the boundary shapes. From engineer's point of view this will undoubtedly broaden the utilization of the shape optimization techniques. A detailed discussion of some mathematical approaches to the choices of finite elements and to the grid optimization for the finite element formulation of structural problems is offered in the paper of A.R. Diaz, N. Kikuchi and J.E. Taylor [14] in this volume. Also see [12] and [8]. For a basic introduction to this topic, see reference [13].

Finally, we comment that the basic problem of pure torsion of an elastic multiply connected bar is an important problem in the theory of elasticity and does have a long history. Large body of literature concerning it goes back to the original papers of Saint Venant, Lord Kelvin (Sir William Thompson) and Prandtl. While the numerical aspects and the theoretical results of this paper dealt with a version of this classical problem or rather with the related problem of shape optimization for elastic multiply connected bars subjected to pure torsion, the uses of material derivative and the other concepts utilized here are quite general and are certainly not restricted to the specific problem stated in the title of this paper.

An elementary introduction to the theory of pure torsion for linear elastic isotropic bars may be found in the reference [1].

REFERENCES

1. Sokolnikoff, I.S., Mathematical Theory of Elasticity, McGraw-Hill, New York, (1956).

2. Polya, G., and Weinstein, A., "On the Torsional Rigidity of Multiply Connected Cross-Sections", Ann. of Math, 52, 154-163, (1950).

3. Banichuk, N.V., "Optimization of Elastic Bars in Torsion", Int. J. Solids Struct., 12, 275-286, (1976).

4. Kurshin, L. M., and Onoprienko, P.N., "Determination of the Shapes of Doubly-Connected Bar Sections of Maximum Torsional Stiffness", Prik. Math. Mech. (English translation Appl. Mathematics and Mechanics, PMM), 40, 1078-1084, (1976).

5. Dems, K., "Multiparameter Shape Optimization of Elastic Bars in Torsion", Int. J. Num. Meth. Engng., 15, 1517-1539, (1980).

6. Aubin, J.P., Applied Functional Analysis, Wiley-Interscience, New York, (1979).

7. Zolesio, J.P., "The Material Derivative (or speed) Method for Shape Optimization", Optimization of Distributed Parameter Structures, Vol. II, (ed, E.J. Haug and J. Cea) Sitjthoff-Noordhoff, Rockville, Md., 1089-1151, (1981).

8. Haug, E.J., Choi, K.K., and Komkov, V., Structural Design Sensitivity Analysis, Academic Press, New York, (1984).

9. Cea, J., "Problems of Shape Optimal Design", Optimization of Distributed Parameter Structures, Vol. II. (ed. E.J. Haug and J. Cea) Sitjthoff-Noordhoff, Rockville, Md., 1005-1048, (1981).

10. Rousselet, B., and Haug, E.J., "Design Sensitivity Analysis of Shape Variation", Optimization of Distributed Parameter Structures, Vol. II, (ed. E.J. Haug and J. Cea) Sijthoff-Noordhoff, Rockville, Md., 1397-1442, (1981).

11. Choi, K.K., Haug, E.J., Hou, J.W., and Sohoni, V.N., "Pshenichny's Linearization Method for Mechanical System Optimization", Trans, ASME, J. Mech. Design, to appear (1984).

12. Pshenichny, B.N., and Danilin, Y.M., Numerical Methods in Extremal Problems, Mir, Moscow, (1978).

13. Zienkiewicz, O.C., The Finite Element Method in Engineering Science, (the second expanded edition), McGraw Hill, London, 1971.

14. Diaz, A.R., Kikuchi N. and Taylor J.E., Optimal Design Formulation for Finite Element Grid Adaptation, in this volume.

LIST OF FIGURES AND TABLES

Table 1. Numerical Results for Optimum Shapes

	Theoretical Values	Optimum Values	
		Coarse Grid	Fine Grid
Torsional Rigidity	1086.44	1067.4	1081.51
Radius of Outer Boundary	5.2016	$5.2625 < b_1 < 5.2716$	$5.2180 < b_1 < 5.2186$
Radius of Inner Boundary	2.523	$2.523 < b_1 < 2.5570$	$2.5312 < b_1 < 2.5313$

Table 2. Numerical Results for a Torsion Bar with Hollow Cross-Section

Given Material	No. of Iterations for Convergence		CPU Seconds on PRIME 750		Optimum Torsional Rigidity		Constraint on Area	
	Coarse Grid	Finer Grid	Coarse Grid	Finer Grid	Coarse Grid	Finer Grid	Coarse Grid	Finer Grid
85 units	704	410	1419.2	1602.7	2457.3	2433.4	83.79	82.9
110 units	755	410	1523.2	1602.7	2826.9	2820.8	107.8	106.7

Table 3. Numerical Results for a Torsion Bar with Solid Cross-Section

Given Material	No. of Iterations for Convergence	CPU Seconds on PRIME 750	Optimum Torsional Rigidity	Constraint on Area
85 units	47	247.4	1139.3	84.99
110 units	177	923.4	1785.2	108.1

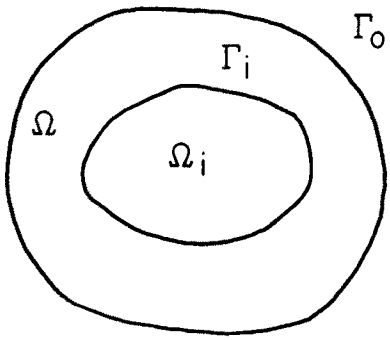

Figure 1. Torsion of a Doubly-Connected Bar

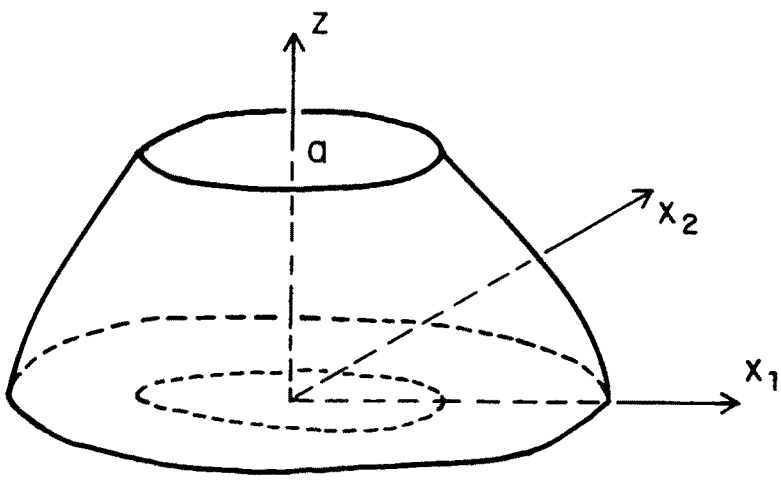

Figure 2. Stress Function for a Doubly-Connected Bar

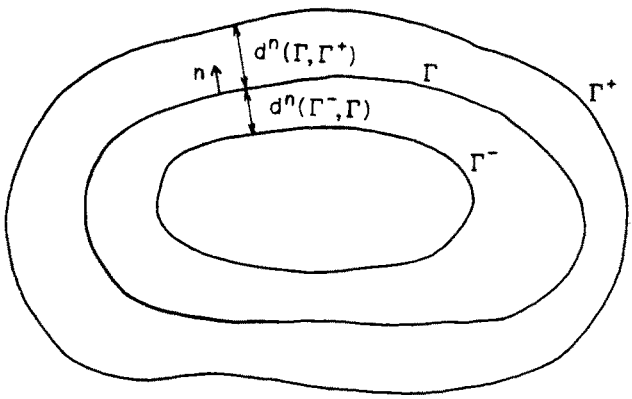

Figure 3. Pointwise Constraint on Boundary Γ

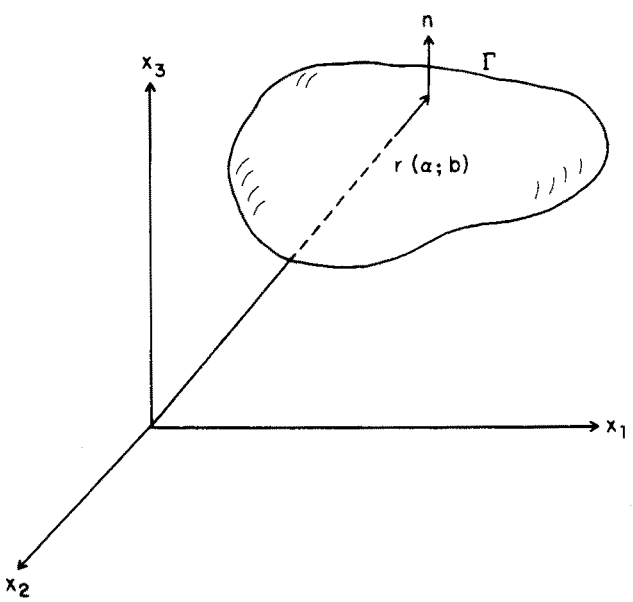

Figure 4. Parametric Definition of Γ

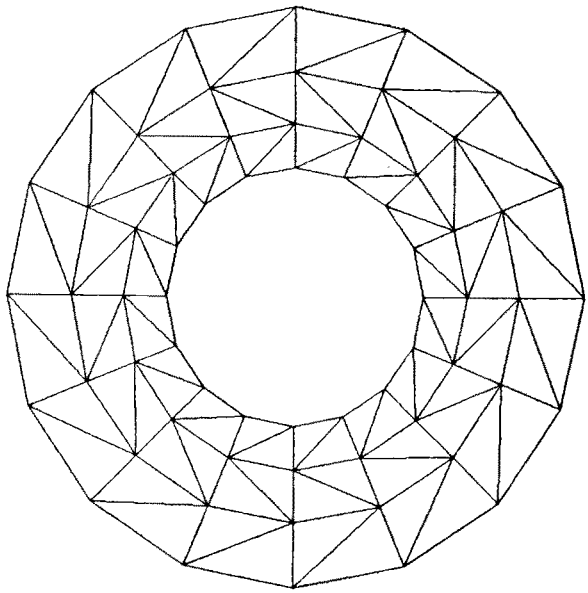

(a) Coarse Grid Model

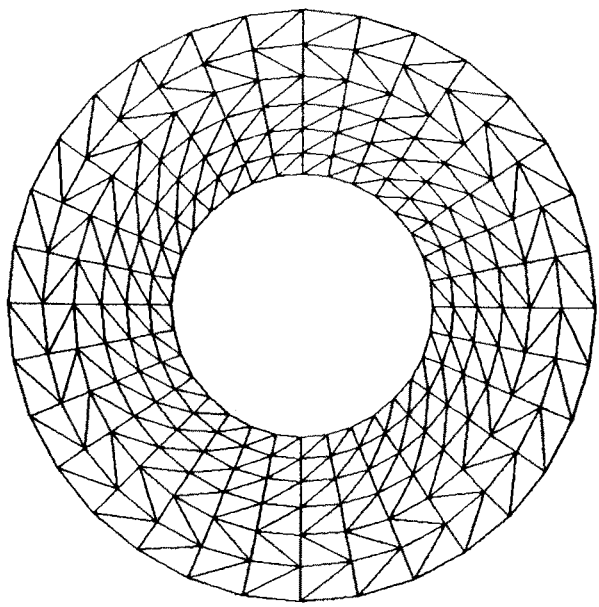

(b) Fine Grid Model

Figure 5. Finite Element Models of Elastic Bar's Cross Section

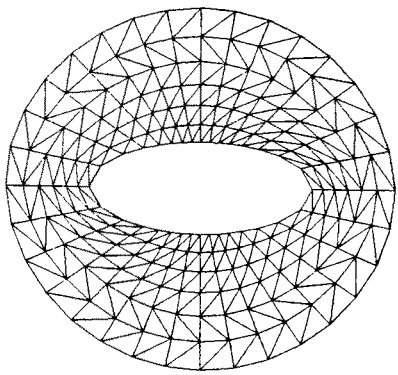

Figure 6. Final Optimum Shape

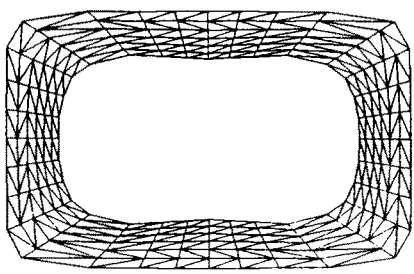

(a) Given amount of material is 85 units

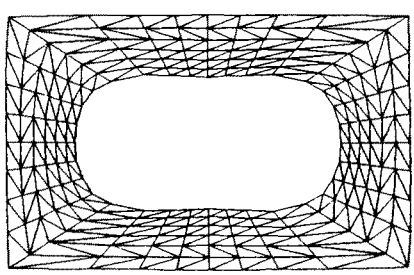

(b) Given amount of material is 110 units

Figure 7. Final Optimum Shapes for a Torsion Bar with Coarse Mesh

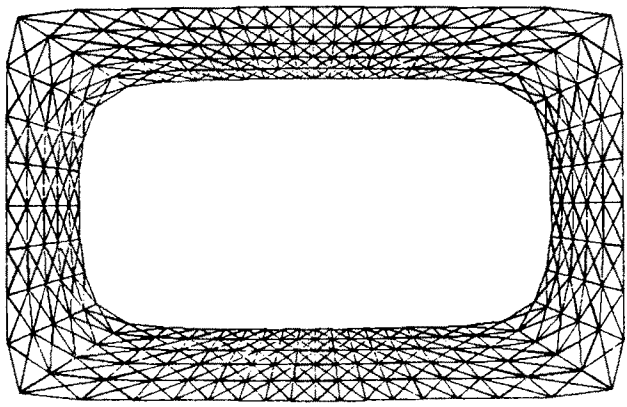

(a) Given amount of material is 85 units

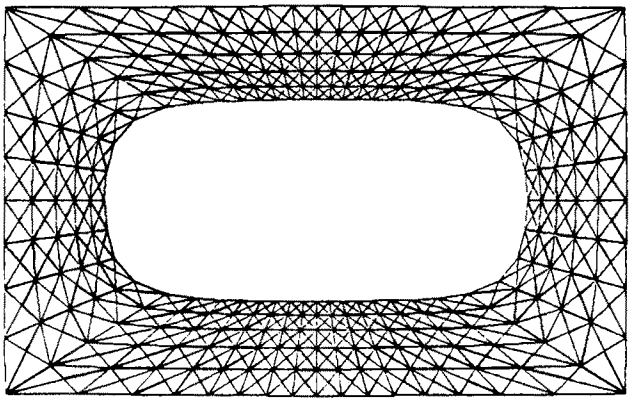

(b) Given amount of material is 110 units

Figure 8. Final Optimum Shapes for a Torsion Bar with Fine Mesh

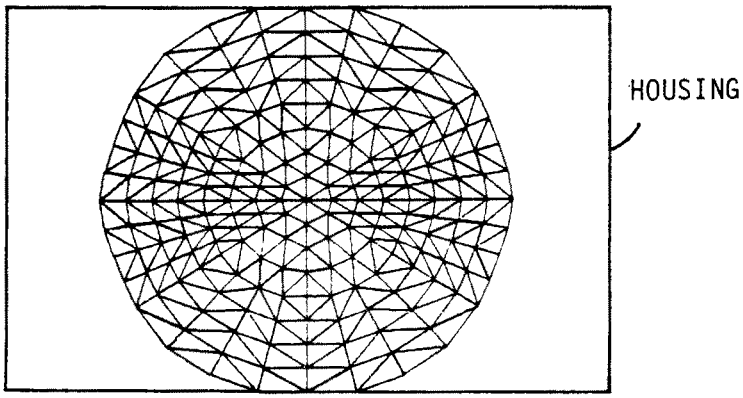

(a) Given amount of material is 85 units

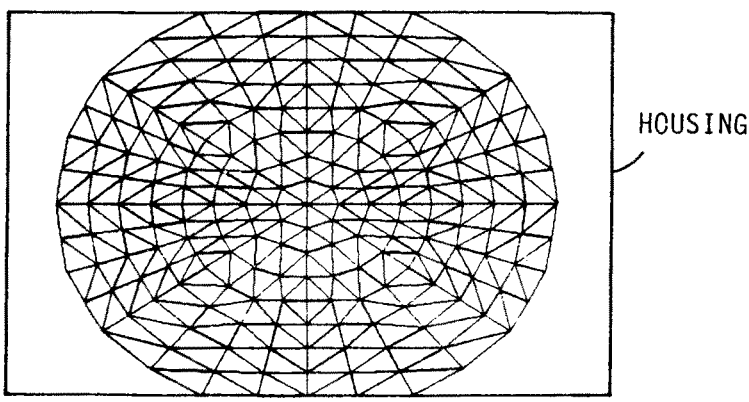

(b) Given amount of material is 110 units

Figure 9. Final Optimum Shapes for a Torsion Bar with Solid Cross-Section